CHAPTER 2

Overview of Computational and Experimental Techniques

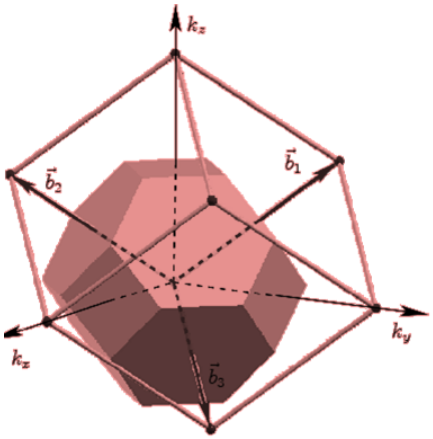

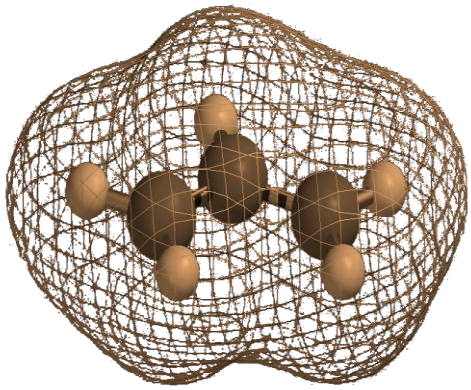

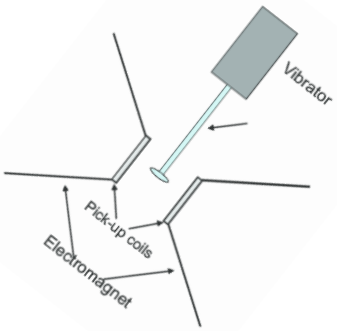

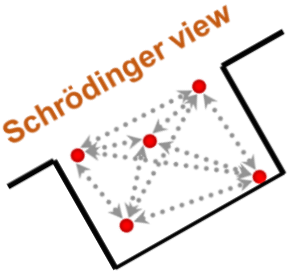

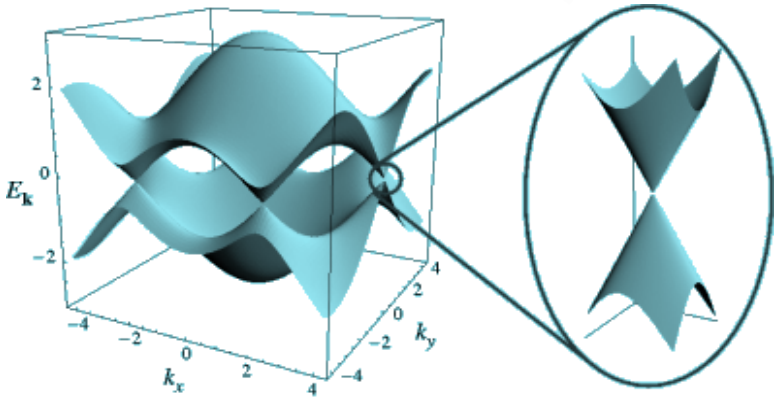

2.1 A summary of Density Functional Theory

The accurate description of the structure and dynamics of many-body systems and the solution of the Schrödinger equation is a complex problem in the field of theoretical physics and computational material science. The basic building blocks of materials are nuclei and electrons. The explanation of the nucleus belongs to classical theory because of the heavy mass as compared to electrons. The strongly localized wave function of the nucleus differs from the electrons which exhibit overlapped orbitals. The interaction of electrons is subjected to both, stationary nuclei in terms of the attractive Coulomb force and the repulsive Coulomb force with neighboring electrons. The interaction phenomenon of electrons specifically makes the electronic structure calculation more complex in terms of many-body problems. To determine the systematic theory for the electronic structure calculations, Hohenberg, Kohn, and Sham established a theory termed density functional theory (DFT). DFT has been recognized for its extraordinary predicting ability despite being independent of experimental input. In the framework of DFT, all the physical quantities are calculated through the self-consisting methodology of solving the quantum mechanical equation. The popularity of DFT has increased and resulted in receiving large appreciation from the theoretical and computational community [1-3].

Crystalline materials are generally considered as many-electron systems with non-distinguishable mutual interaction in a lattice composed of nuclei. The effective potential in the Schrödinger equation includes Coulomb potential (because of the electronic charge distribution which is termed as Hartree potential) and exchange-correlation potential. The term exchange potential is based on the Pauli's exclusion principle and the correlations term originates due to the effect of a single electron on the overall charge distribution of the system. In the formulation of DFT, the electron density distribution function $n(r)$ is used instead of

many electron wave functions $\Psi(r_1,\ r_2,\ r_3 \ldots\ldots\ldots r_N)$ to determine the ground state energy *E* for any system consisting of N nuclei and electrons [4]. This reduces the solution of many body problem to that of single-particle Schrödinger equation with ground-state density distribution. Any crystalline material can be treated as a system of heavy nucleus and electrons interacting with each other based on quantum mechanics. The ground state energy of this system can be evaluated by solving the corresponding many-body Schrödinger equation [5]:

$$H\psi = E\psi \tag{2.1}$$

where H is the many particle Hamiltonian, ψ is the many-body wave function and E is the ground state total energy. In the case of a hydrogen (H) atom which possesses one electron and one proton, one can solve the above equation exactly for an H atom with the calculated energy of -13.6 eV. However, for the crystal structures with many electrons and ions system, it is treated with complex interactions of the electron and ions. The Hamiltonian for such a system of interacting electrons and nuclei can be written as follows:

$$\hat{H} = \hat{T}_N + \hat{T}_E + \hat{V}_{EE} + \hat{V}_{EN} + \hat{V}_{NN} \tag{2.2}$$

were $\hat{T}_N$ and $\hat{T}_E$ are the kinetic energy operator for the nuclei and electrons respectively, $\hat{V}_{EE}$, $\hat{V}_{EN}$ and $\hat{V}_{NN}$ are the electrostatic potential energy operators for electron-electron, nuclei-nuclei, and the electrons-nuclei interactions respectively. The many body Schrödinger equation can be rewritten as:

$$H\psi = \left[-\frac{\hbar^2}{2m_e}\sum_i \frac{\partial^2}{\partial \bar{r}_i{}^2} - \frac{\hbar^2}{2M}\sum_k \frac{\partial^2}{\partial \bar{R}_k{}^2} + \frac{1}{2}\sum_{\substack{k,k' \\ k\neq k'}} \frac{e^2}{4\pi\varepsilon_0}\frac{Z_l Z_{l'}}{|\bar{R}_k - \bar{R}_{k'}|} + \frac{1}{2}\sum_{\substack{i,j \\ i\neq j}} \frac{e^2}{4\pi\varepsilon_0}\frac{1}{|\bar{r}_i - \bar{r}_j|} - \right.$$

$$\left.\sum_i \sum_k \frac{e^2}{4\pi\varepsilon_0}\frac{Z_l}{|\bar{r}_i - \bar{R}_k|}\right]\psi = E\psi \tag{2.3}$$

where i, k are the indices consecutively for electron and nuclei, m_e, M are the mass of electron and nuclei respectively, Z_k, $Z_{k'}$ defines the charges on different nuclei, $\bar{\boldsymbol{r}}_{\boldsymbol{i}} - \bar{\boldsymbol{r}}_{\boldsymbol{j}}$, $\bar{\boldsymbol{R}}_{\boldsymbol{k}} - \bar{\boldsymbol{R}}'_{\boldsymbol{k}}$, $\bar{\boldsymbol{r}}_{\boldsymbol{i}} - \bar{\boldsymbol{R}}_{\boldsymbol{k}}$ are the distances between electron-electron, nuclei-nuclei, and electron-nuclei respectively. The solution of Equation 2.1 gives the energy eigenstates i.e., the total energy of the system. Hence, the solution of the above equation is computationally costly and the solution is

computationally feasible only for simple systems. Therefore, some approximation is essential to determine the properties of the complex systems.

2.2 Wave Function-based Methods to Solve Many-body Problem

2.2.1 The Born-Oppenheimer Approximation

Born-Oppenheimer approximation [6] exploits the fact that the nucleus is heavier as compared to the electrons ($M_n \gg m_e$). Therefore, the kinetic energy of the nuclei is very less than the moving electrons. Further, the assumption is based on the idea that the nuclei is static with respect to the moving electrons thus their kinetic energy can be neglected. Hence the wave function can be simplified into two parts i. e., the electronic part and ionic part leading to many-body wave functions as:

$$\psi = \chi_l(\bar{R})\, \phi_i(\bar{r},\, \bar{R}) \tag{2.4}$$

Here $\chi_l(\bar{R})$ denotes ionic, and $\phi_i(\bar{r},\, \bar{R})$ represents the electronic wave function. Thus, the simplified form of equations based on the ionic and electronic wave function is written as:

$$\left[-\frac{\hbar^2}{2M}\sum_l \frac{\partial^2}{\partial \bar{R}_k^{\,2}} + V_{II}(\bar{R}) + E_E(\bar{R})\right]\chi_k(\vec{R}) = E\chi_k(\bar{R}) \tag{2.5}$$

$$\left[-\frac{\hbar^2}{2m_e}\sum_i \frac{\partial^2}{\partial \bar{r}_i^{\,2}} + V_{IE}(\bar{r},\, \bar{R}) + V_{EE}(\bar{r})\right]\, \phi_i(\bar{r},\, \bar{R}) = E_E\, \phi_i(\bar{r},\, \bar{R}) \tag{2.6}$$

where $\bar{r} = \bar{r}_1, \bar{r}_2, \bar{r}_3, ..$ and $\bar{R} = \bar{R}_1, \bar{R}_2, \bar{R}_3,$ represents a collective symbol for electronic and ionic coordinate respectively. The first term of Equation 2.2 vanishes under Born-Oppenheimer (BO) approximation and the last term will be a constant [7]. The resulting Hamiltonian can be written as:

$$\hat{H} = \hat{T}_E + \hat{V}_{EE} + \hat{V}_{EN} + \text{Constant} \tag{2.7}$$

The Hamiltonian operator can be written as the sum of the kinetic energy of electrons ($\hat{T}_E$), the interaction between the electron-electron (V_{EE}) and the interaction with the external potential (V_{ext})

$$\hat{H} = \hat{T}_E + \hat{V}_{EE} + \hat{V}_{ext} \tag{2.8}$$

where the electron kinetic energy operator $\hat{T}_E$ is given as

$$\hat{T}_E = \frac{-\hbar^2}{2m_e}\sum_i \frac{\partial^2}{\partial \bar{r}_i^2} \tag{2.9}$$

and the potential due to electron-electron interactions V_{EE} is:

$$\hat{V}_{EE} = \frac{1}{2}\sum_{i\neq j} \frac{e^2}{|r_i - r_j|} \tag{2.10}$$

The external potential of the electron-nuclei interactions is defined as:

$$\hat{V}_{ext} = \sum_{i,I} V(|r_i - R_I|) \tag{2.11}$$

were r_i is the coordinate of i^{th}electron and V is the external potential.

2.2.2 Hartree Approximation

Hartree approximation is based on the fact that electron-electron interaction possesses its stability following classical electrostatics and the Coulomb repulsion. The distribution of electronic charge $n(r)$ yields an electrostatic potential through Poisson's equation given by;

$$\nabla^2\varphi(r) = 4\pi n(r) \tag{2.12}$$

The potential energy called Hartree potential $V_H(r)$ which satisfies the Poisson's equation [8] is given as:

$$\nabla^2 V_H(r) = -4\pi n(r) \tag{2.13}$$

Equation 2.9 transforms in Hartree units and the potential energy $V_H(r) = -\varphi(r)$, known as Hartree potential. Utilizing the Hartree potential, the complete Schrödinger equation for the electronic part can be written as:

$$-\frac{\hbar^2}{2m_e}\nabla_i{}^2\phi_i - \frac{1}{4\pi\varepsilon_0}\sum_k \frac{Z_k e^2}{|\bar{r}_i - \bar{R}_k|}\phi_i + \frac{1}{4\pi\varepsilon_0}\sum_{j\neq i}\int \frac{e^2|\Psi_j|^2}{|\bar{r}_i - \bar{r}_j|} d^3 r_j = E_i\phi_i \tag{2.14}$$

The equation can be simplified in three parts, first is the kinetic energy of electrons (first term), the second is ion-electron interaction depending on the position of the electron and the last term represents the Hartree potential. The solution of the Hartree equation (Equation 2.14) is given by the variational principle that estimates the energy by minimizing the expectation value of energy E.

$$E = \frac{\langle \Psi_H | H | \Psi_H \rangle}{\langle \Psi_H | \Psi_H \rangle} \tag{2.15}$$

Hartree reduced many-body problems into one electron problem which is also known as independent electron approximation which neglected correlations between electrons and the asymmetric wave function for electrons.

2.2.3 Hartree-Fock (HF) Approximation

Since electrons are fermions and follow Pauli's exclusion principle, the asymmetric nature of wave function and the effect of correlation cannot be ignored. Hartree and Fock considered the asymmetric wave function given by the equation below:

$$\Psi_{HF}(\bar{r_1}, \sigma_1, \dots, \bar{r_i}, \sigma_i, \ \dots, \bar{r_j}, \sigma_j, \dots) = -\Psi_{HF}(\bar{r_1}, \sigma_1, \dots, \bar{r_i}, \sigma_i, \ \dots, \bar{r_j}, \sigma_j, \dots) \tag{2.16}$$

In HF approximations, the minimization of Equation 2.14 is done by considering the above asymmetric wave function in the determinant form known as Slater's determinant [9].

$$\Psi_{HF}(\bar{r_1}, \sigma_1, \dots, \bar{r_N}, \sigma_N) = \begin{vmatrix} \Psi_1(\bar{r_1}, \sigma_1) & \Psi_1(\bar{r_2}, \sigma_2) \dots & \Psi_1(\bar{r_N}, \sigma_N) \\ \Psi_2(\bar{r_2}, \sigma_2) & \Psi_2(\bar{r_2}, \sigma_2) \dots & \Psi_2(\bar{r_N}, \sigma_N) \\ \Psi_N(\bar{r_N}, \sigma_N) & \Psi_N(\bar{r_N}, \sigma_N) \dots & \Psi_N(\bar{r_N}, \sigma_N) \end{vmatrix} \tag{2.17}$$

The determinant of the wave function can be written as

$$\Psi_{HF} = \frac{1}{N!} \sum_P (-1)^p P \, \Psi_1(x_1) \, \Psi_2(x_2) \dots \Psi_N(x_N) \tag{2.18}$$

where $x = (\bar{r_i}, \sigma)$, P is the permutation number and p is the number of interchanges for making up this permutation. Substituting the Slater determinant of many body wave function in Equation 2.14 gives the expectation value of Hamiltonian as

$$E = \sum_i \int \Psi_i^*(\vec{r}) \left[-\frac{\hbar^2}{2m_e} \sum_i \nabla_i^2 + V_I(\vec{r}) \right] \Psi_i(\vec{r}) d^3r + \frac{1}{2} \sum_i \sum_{i \neq j} \iint \frac{e^2}{4\pi\varepsilon_0} \frac{|\Psi_i(x_i)|^2 |\Psi_j(x_j)|^2}{|\vec{r} - \vec{r}'|} d^3r d^3r'$$

$$- \frac{1}{2} \sum_{i,j} \sum_{j \neq i} \iint \frac{e^2}{4\pi\varepsilon_0} \frac{\Psi_i^*(\vec{r}) \Psi_j^*(\vec{r}') \Psi_i(\vec{r}') \Psi_j(\vec{r})}{|\vec{r} - \vec{r}'|} d^3r d^3r' \quad (2.19)$$

where the last term is the consequence of Pauli's exclusion principle known as exchange energy. Minimization of Equation 2.19 leads to Hartree-Fock equation

$$\left[-\frac{\hbar^2}{2m_e} \sum_i \nabla^2 - V_I(\vec{r}) + V_H(\vec{r}) \right] \Psi_i(\vec{r}) - \frac{1}{2} \sum_{i,j} \sum_{j \neq i} \iint \frac{e^2}{4\pi\varepsilon_0} \frac{\Psi_j^*(\vec{r}') \Psi_i(\vec{r}') \Psi_j(\vec{r})}{|\vec{r} - \vec{r}'|} d^3r d^3r' = E_i \Psi_i(\vec{r}) \quad (2.20)$$

This is an improvement over the Hartree method due to the involvement of exchange energy considering the asymmetric nature of wave-function. However, total energy E_i involves minimization over the sum of N particle Slater's determinant (Equation 2.17) and this type of determinant are quite large, hence this approximation becomes computationally very costly for large as well as small systems.

2.3 Density Based Method; Density Functional Theory

The basic purpose is to calculate the ground state energy of many electron systems through solving many body Schrödinger equation given in Equation 2.3. For a system with N electrons, there exist 3N variables leading to the complex solution of Equation 2.3. The DFT depends on a density-based method where the interaction energy and potentials depend only on the density of electrons which decreases the computational cost.

2.3.1 Hohenberg and Kohn Theorem

Hohenberg and Kohn built the basis of DFT based on two theorems.

Theorem I: For any system of interacting particles in an external potential $V_{ext}(\mathbf{r})$, the potential $V_{ext}(\mathbf{r})$ is determined uniquely, except for a constant, by the ground state particle density **n(r).”** [10-12]

Theorem II: The function that delivers the ground state energy of the system, describes the lowest energy if and only if the input density is the true ground state density.

2.3.2 The Kohn-Sham Equation

The Kohn-Sham perturbed DFT into a practical tool by the construction of an auxiliary system of non-interacting quasiparticles that have the density same as that of the true interacting problem.. If there exist a system of non-interacting electrons with the same density as of interacting system, according to the Hohenberg-Kohn theorem, the total energy for the interacting system can be written as:

$$E[n] = T[n] + V[n] + \int V_{ext}(r) n(r) d^3r \tag{2.21}$$

where T[n], V[n] and $V_{ext}(r)$ are the kinetic energy functional, Coulomb potential functional and external potential respectively. Since the single-particle system and the interacting system are assumed to have the same density, adding and subtracting $T_s[n]$ (the non-interacting kinetic energy) and $E_H[n]$ (the Hartree energy) to (2.21), gives

$$E_{KS}[n] = T_s[n] + E_H[n] + \{T[n] - T_s[n] + V[n] - E_H[n]\} + \int V_{ext}(r) n(r) d^3r \tag{2.22}$$

$$E_{KS}[n] = T_s[n] + E_H[n] + E_{xc}[n] + \int V_{ext}(r) n(r) d^3r \tag{2.23}$$

where the exchange-correlation energy is defined as:

$$E_{xc}[n] = T[n] - T_s[n] + V[n] - E_H[n] \tag{2.23}$$

where the difference in kinetic energy $T[n]-T_s[n]$ is the kinetic contribution to correlation and the difference $V[n]-E_H[n]$ is the electrostatic and exchange contribution to correlation. Though the exchange-correlation potential spans all important quantum many-body effects, the evaluation of exact exchange-correlation functional is very challenging. Therefore, approximations are done by simple functionals as discussed in Section 2.3.3. The non-interacting kinetic energy T_s density $n(r)$ and particle count N of the non-interacting system can be evaluated from the single-particle wave functions as:

$$T_s[n] = -\frac{1}{2}\sum_{i}^{N} \left\langle \psi_i \middle| \nabla^2 \middle| \psi_i \right\rangle \tag{2.24}$$

$$n(r) = \sum_{i}^{N} |\psi_i(r)|^2 \tag{2.25}$$

$$N = \int n(r) d^3 r \tag{2.26}$$

$T_s[n]$ is explicitly expressed as a functional of the orbitals whereas all other terms are functionals of the density, the solution of Equation 2.23 is the problem of minimization with respect to density *n(r)*.

$$\frac{\delta E_{KS}}{\delta \psi_i^*(r)} = \frac{\delta T_s[n]}{\delta \psi_i^*(r)} + \left[\frac{\delta E_{ext}[n]}{\delta n(r)} + \frac{\delta E_H[n]}{\delta n(r)} + \frac{\delta E_{xc}[n]}{\delta n(r)}\right] \frac{\delta n(r)}{\delta \Psi_i^*(r)} = 0$$

(2.27)

From Equation (2.24) and (2.25):

$$\frac{\delta T_s[n]}{\delta \psi_i^*(r)} = -\frac{1}{2}\nabla^2 \psi_i(r) \quad \text{and} \quad \frac{\delta n(r)}{\delta \psi_i^*(r)} = \psi_i(r) \tag{2.28}$$

which leads to the KS Schrödinger like equations:

$$(H_{KS} - E_i)\psi_i(r) = 0 \tag{2.29}$$

where the ε_i are the eigenvalues, and H_{KS} is the effective Hamiltonian

$$H_{KS}(r) = -\frac{1}{2}\nabla^2 + V_{KS}(r) \tag{2.30}$$

$$V_{KS}(r) = V_{ext}(r) + V_H(r) + V_{xc}(r) \tag{2.31}$$

Equations (2.29)-(2.31) are the well-known Kohn-Sham equations, where the total energy E_{KS} and density n(r) are given by (2.23) and (2.26). These are independent particle equations and the potential can be found using the density self consistently. The exact ground state density and energy can be obtained if exact functional $E_{xc}[n]$ is known.

2.3.3 Exchange and Correlation Functionals

Framing a good approximation for exchange correlation energy (E_{xc}) is an active field of research. There are different functionals available for any particular system which shows valid results with theory and experimental data. The typically used approximations are the local density approximation (LDA) and the generalized gradient approximation (GGA). In local density approximation (LDA), the functional is implicit to have a dependence on the electron

density of homogeneous electron gas (HEG). It depends on the electron density [13] and is based on the uniform homogeneous electron gas (HEG). In LDA, the exchange of uniform electron gas of a density equals to the density at the point where the exchange is to be assessed is used:

$$E_{xc}^{LDA}[n] = -\frac{3}{4\pi}\left(3\pi^2\right)^{1/3}\int n^{4/3}(r)d^3r \tag{2.32}$$

However, a serious limitation of LDA is that it cannot provide an estimation of the long-ranged Van der Waals (vdW) interaction. Generalized gradient approximation (GGA) is a modification over LDA where first-order gradient terms are included such that the exchange-correlation energy is dependent on the local densities and their gradients [14]. The functionals are defined in generalized form as:

$$E_{xc}^{GGA}[n^{\uparrow}, n^{\downarrow}] = \int n(r)\,\varepsilon_{xc}\left(n^{\uparrow}, n^{\downarrow}, \left|\nabla n^{\uparrow}\right|, \left|\nabla n^{\downarrow}\right|\right)d^3r \tag{2.33}$$

$$E_{xc}^{GGA}[n^{\uparrow}, n^{\downarrow}] = \int n(r)\,\varepsilon_{x}^{hom(n)_{xc}\left(n^{\uparrow}, n^{\downarrow}, \left|\nabla n^{\uparrow}\right|, \left|\nabla n^{\downarrow}\right|\right)^3} \tag{2.34}$$

where F_{xc} is a dimensionless quantity and $\varepsilon_x^{\text{hom}}(n)$ is the exchange energy. Many studies have demonstrated that the GGA improves the LDA error in calculating cohesive energies of solids and molecules [15].

2.4 Density Functional Perturbation Theory

Many physical properties depend upon a system response to some sort of perturbation. Examples include polarizabilities, phonons, Raman intensities, and infra-red absorption cross-sections. Density functional perturbation theory (DFPT) is a particularly powerful and flexible theoretical technique that allows calculation of properties such as calculate response function, phonon frequencies and Born effective charges [16-18] within the density functional framework, thereby facilitating an understanding of the microscopic quantum mechanical mechanisms behind such processes, as well as providing a rigorous testing ground for

theoretical developments. In DFPT, V, E, H, Ψ_{kn}, n(r), etc. are subjected to perturbation. The external potential V is expanded as

$$V_{ext} = V_{ext}^{0} + \lambda V_{ext}^{(1)} + \lambda^2 V_{ext}^{(2)} + \lambda^3 V_{ext}^{3} + \ldots\ldots \quad (2.35)$$

Similar expansions are done for E, H, Ψ_{kn}, n(r), etc. The second-order energy $E^{(2)}$, is an important parameter that is used to calculate the dynamical matrix for phonon calculations and Born effective charges. One can write energy as functional of density as:

$$E[n] = \min_{\psi^{(1)}} \sum_{i\in occ} \langle \psi_i | T + V_{ext} | \psi_i \rangle + E_{Hxc}[n] \quad (2.36)$$

$$E^{(2)} = \min_{\psi^{(1)}} \sum_{i\in occ} \left[\left\langle \psi_i^{(1)} \middle| H^{(0)} - \varepsilon_i^{(0)} \middle| \psi^{(1)} \right\rangle + \left\langle \psi_i^{(1)} \middle| V_{ext}^{(1)} \middle| \psi_i^{(0)} \right\rangle + \left\langle \psi_i^{(0)} \middle| V_{ext}^{(1)} \middle| \psi^{(1)} \right\rangle + \left\langle \psi_i^{(0)} \middle| \upsilon_{ext}^{(2)} \middle| \psi_i^{(0)} \right\rangle \right] + \frac{1}{2} \frac{\delta^2 E_{Hxc}}{\delta n(r) \delta n(r')} \Big| n^{(0)} n^{(1)}(r) n^{(1)}(r') d^3 r d^3 r' + \int \frac{d}{d\lambda} \frac{\delta E_{Hxc}}{\delta n(r)} \Big|_{n^{(0)}} n^{(1)}(r) d^3(r) \frac{1}{2} \frac{d^2 E_{Hxc}}{d\lambda^2} \Big|_{n^{(0)}} \quad (2.37)$$

where the second-order term of energy is obtained as variational with respect to first order wave function provided first order wavefunctions are orthogonal to the ground state wavefunctions

$$\left\langle \psi_i^{(0)} \middle| \psi_j^{(j)} \right\rangle = 0 \quad (2.38)$$

The dynamical matrices are Hermitian and the eigenvalues $\omega_j{}^2(q)$ are real with eigenvectors $\xi_j(q)$ being orthonormal. Also, the phonon band structure $\omega_j(q)$ directly corresponds to density of states (DoS) which provides the information of phonons in the whole Brillouin Zone (BZ). To obtain the information of the whole phonon spectrum, the scanning of BZ is important. This scanning consists in matrix diagonalization over the three-dimensional grid of wave vector $\boldsymbol{q} = \left(\frac{a^*}{n_1}, \frac{b^*}{n_2}, \frac{c^*}{n_3}\right)$, at n_1, n_2, n_3 = -N,., N. In total, this includes $N_i = (2N + 1)^3$ points

in BZ. The phonon density of states (PHDOS) is determined by summation over all the phonon states and is defined by:

$$g(\omega) = D' \int_{BZ} \sum_j \delta\left(\omega - \omega_j(q)\right) dq = D' \int_{BZ} \sum_{jp} \delta\left(\omega - \omega_j(q)\right) dq_p \quad (2.39)$$

Here, D' is a normalization constant such that $\int g(\omega) d\omega = 1$; and $g(\omega)d\omega$ is the fraction of phonons with energies ranges from ω to $\omega + d\omega$. The mesh index 'p' is characterized by 'q' in the discretized irreducible Brillouin zone, where $d\boldsymbol{q}_p$ provides the weighting factor corresponding to the volume of p^{th} mesh in $\boldsymbol{q}$-space. The phonon density of states (PHDOS) can be described as:

$$g(\omega) = D' \sum_{jp} \delta\left(\omega - \omega_j(q)\right) \frac{|\xi_j(q)|^2}{\sum_{jp} |\xi_j(q)|^2} \quad (2.40)$$

2.5 Elastic Properties

The mechanical properties of crystalline material are defined in terms of elastic constants and further characterized by Young's modulus, shear modulus, bulk modulus, and Poisson's ratio. Elastic properties also govern the thermodynamic properties such as specific heat, thermal expansion, and Debye temperature [19]. The total energy of a strained system E_{tot} having volume V can be expressed as:

$$E_{tot} = E^0_{tot} + P(V - V_0) + \Phi_{elast} \quad (2.41)$$

where E^0_{tot} is the total energy of crystal at initial stage with volume V_0 without strain. Φ_{elast} is the elastic energy and P is the pressure defined by:

$$P = -\left(\frac{\partial E^0_{tot}}{\partial V}\right)(V_0) \quad (2.42)$$

The elastic constants (C_{ijkl}) can be defined using elastic energy Φ_{elast} following Hooke's law as:

$$\Phi_{elast} = \frac{V}{2} C_{ijkl} \varepsilon_{ij} \varepsilon_{kl} \quad (i, j, k, l = 1, 2, 3) \quad (2.43)$$

or, in the Voigt's suffix notation:

$$\Phi_{elast} = \frac{V}{2} C_{ij} \varepsilon_i \varepsilon_j \qquad (i, j = 1, 2, 3, 4, 5, 6) \tag{2.44}$$

Since in Equation (2.41), the (V-V_0) term follows linear relationship with strain, it is possible to derive elastic constants from the second order derivatives of E_{tot}:

$$C_{ij} = \frac{1}{V_0} \frac{\partial^2 E_{tot}}{\partial \varepsilon_i \partial \varepsilon_j} \tag{2.45}$$

Elastic tensor of cubic crystal has only three independent elastic constants, C_{11}, C_{12}, and C_{44}:

$$C = \begin{pmatrix} C_{11} & C_{12} & C_{12} & & & \\ C_{12} & C_{11} & C_{12} & & & \\ C_{12} & C_{12} & C_{11} & & & \\ & & & C_{44} & & \\ & & & & C_{44} & \\ & & & & & C_{44} \end{pmatrix} \tag{2.46}$$

All the three elastic constants of a cubic crystal can be determined by solving three equations implying that three types of strain must be applied to the crystal. The bulk modulus of crystal can be evaluated by fitting $E_{tot}(V)$ with the third order Birch-Murnaghan [20] equation of state where the E_{tot} is computed for different values of strain. To evaluate the elastic tensors, volume conservative tetragonal strains are applied where one varies the axial ratio $\frac{c}{a} = 1 + e$ leading to the strain tensor:

$$\bar{\varepsilon} = \begin{pmatrix} \varepsilon_1 & 0 & 0 \\ 0 & \varepsilon_1 & 0 \\ 0 & 0 & \frac{1}{(1+\varepsilon_1)^2} - 1 \end{pmatrix} \text{ or in Voigt notation } \begin{pmatrix} \varepsilon_1 \\ \varepsilon_1 \\ \frac{1}{(1+\varepsilon_1)^2} - 1 \\ 0 \\ 0 \\ 0 \end{pmatrix} \tag{2.47}$$

where $\varepsilon_1 = (1 + e)^{-1/3} - 1$. The elastic energy resulting from tetragonal strain to second order in ε_1 can be written as:

$$\frac{\Phi_{tetra}}{V_0} = 3(C_{11} - C_{12})\varepsilon_1^2 + o(\varepsilon_1^3) \tag{2.48}$$

E_{tot} (ε_l) is fitted to an N degree polynomial P which is decided by the number of deformed structures ($N \leq$ (Number of data) - 1). The value of (C_{11}-C_{12}) is obtained from computing the second derivative of P:

$$P''(\varepsilon_1 = 0) = 6V_0(C_{11} - C_{12}) \quad (2.49)$$

The mechanical stability of a system can be studied by evaluating elastic constants from the ground state total energy calculations. A given crystal cannot exist in a stable or metastable phase if their elastic constants does not follow the stability criteria determined by themselves. The mechanical stability criteria [21-22] for cubic crystals at ambient conditions are:

$$C_{11} + 2C_{12} > 0, C_{44} > 0, C_{11} - C_{12} > 0, C_{11} < B < C_{11}, \quad (2.50)$$

and the isotropic bulk modulus (B) is given by:

$$B = \frac{1}{3}(C_{11} + 2C_{12}) \quad (2.51)$$

The Born criteria for 2D hexagonal structure [23] are:

$$C_{11} > 0,\ C_{11}\text{-}C_{12} > 0 \text{ and } C_{66} > 0 \quad (2.52)$$

The elastic modulus characterized by the Young's modulus (E), shear modulus (G_H), Poisson's ratio (σ) [24] play an important part in determining the strength of the material. They are calculated using the following relations:

$$E = \frac{9BG_H}{3B+G_H} \quad (2.53)$$

$$G_H = \frac{G_V+G_R}{2} \quad (2.54)$$

$$\sigma = \frac{3B-2G}{2(3B+G)} \quad (2.55)$$

where Voigt shear modulus is:

$$G_V = \frac{C_{11}-C_{12}+3C_{44}}{5} \quad (2.56)$$

and Reuss shear modulus is:

$$G_R = \frac{5C_{44}(C_{11}-C_{12})}{4C_{44}+3(C_{11}-C_{12})} \quad (2.57)$$

2.6 Optical Properties

The optical properties such as dielectric constant, absorption coefficient, reflectivity, refractive index, and loss function, etc. describe the interaction of light with the system, useful

in optoelectronic devices. Optical properties of a system can be measured by the complex dielectric function (CDF). The real part ($\varepsilon_1(\omega)$) of the dielectric function can be determined by Kramer–Kroning transformation within the random phase approximation (RPA). The CDF is used to measure the linear response to an external electromagnetic field with a small wave vector k, the optical properties can be derived from the same [25-26]. Expressions for the absorption coefficient, refractive index, coefficient of extinction, optical reflectivity and loss spectra are given as follows:

$$\varepsilon(\omega) = \varepsilon_1(\omega) + i\,\varepsilon_2(\omega) \tag{2.58}$$

The imaginary part ($\varepsilon_2(\omega)$) of the dielectric function can be determined using electronic band structure through the momentum matrix element and the joint density of states (JDOS) between the unoccupied and occupied wave functions within the selection rules and is given by:

$$\varepsilon_2(\omega) = \frac{2e^2\pi}{\Omega\,\varepsilon_0}\sum_{k,c,v}\int |\psi_k^c < \hat{u}\times r > \psi_k^v|^2\,\delta(E_k^c - E_k^v - E) \tag{2.59}$$

The imaginary part of the dielectric function in the above equation depends on JDOS and momentum matrix element. The Kramer–Kronig relation is used to calculate $\varepsilon_1(\omega)$ from $\varepsilon_2(\omega)$ of the dielectric function [27] as:

$$\varepsilon_1(\omega) = 1 + \frac{2}{\pi}P\int \frac{\omega'\varepsilon_2(\omega')}{\omega'^2-\omega^2}d\omega' \tag{2.60}$$

The absorption coefficient $\alpha(\omega)$ is obtained directly from the dielectric function $\varepsilon(\omega)$,

$$\alpha(\omega) = \frac{\sqrt{2\omega}}{c}[\sqrt{(\varepsilon_1^2 + \varepsilon_2^2 - \varepsilon_1}]^{\frac{1}{2}} = \alpha = \frac{2\omega k}{c} = \frac{4\pi k}{\lambda_0} \tag{2.61}$$

where, c is the speed of light. As mentioned above, all the other optical parameters can be calculated by the Equations (2.59) and (2.60).

$$k(\omega) = \frac{1}{\sqrt{2}}[(\varepsilon_1^2 + \varepsilon_2^2)^{\frac{1}{2}} - \varepsilon_1]^{1/2} \tag{2.62}$$

$$n(\omega) = \frac{1}{\sqrt{2}}[(\varepsilon_1^2 + \varepsilon_2^2)^{\frac{1}{2}} + \varepsilon_1]^{1/2} \tag{2.63}$$

In these equations $k(\omega)$ and $n(\omega)$ represent the extinction coefficient and refractive index respectively. The Equation (2.63) is used to determine the reflectivity($R(\omega)$), and given by

$$R(\omega) = \frac{[(n-1)^2+k^2]}{[(n+1)^2+k^2]} \quad (2.63)$$

Now, to calculate the energy loss by an electron in the semiconductors, we have calculated the loss function $L(\omega)$, which is given by

$$L(\omega) = \frac{\varepsilon_2(\omega)}{\varepsilon_1^2(\omega)+\varepsilon_2^2(\omega)} \quad (2.64)$$

2.7 Experimental Techniques

In this section, the details of the solid-state synthesis method and the optimization to prepare the samples are described. To analyze the correlation of the samples with their structural properties, the characterization methods employed are, X-ray Diffraction (XRD) for structural properties, X-ray photoelectron spectroscopy (XPS) for the determination of oxidation states and chemical bonding, Vibrating Sample Magnetometer (VSM) for the study of magnetic properties and Raman spectra for vibrational properties.

2.7.1 Sample Preparation

The polycrystalline powder samples of pristine $CuCoO_2$ and vanadium doped $CuCo_{1-x}V_xO_2$ at different concentrations were synthesized by solid-state synthesis technique (see Fig. 2.1). Stoichiometric amounts of the powders Cu_2O (99.99%), Co_2O_3 (99.9%), and V_2O_5 (99.9%) were mixed and grilled in an agate mortar to ensure homogeneity. A homogenous mixture was obtained in powder form. The resulting mixture was calcinated at 1200 ℃ in the air for 15 h. The calcined powders were then quenched to room temperature.

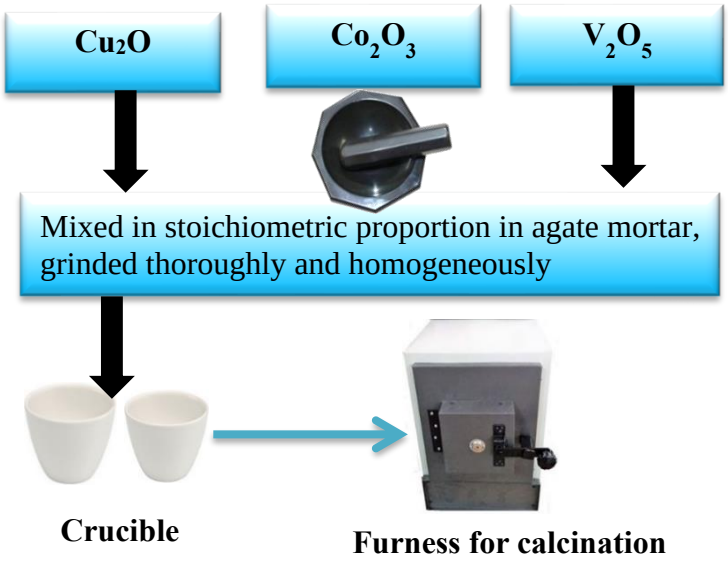

Figure 2.1: Schematic representation of the sample preparation methodology.

2.7.2 Characterization Techniques

A. X-ray Diffraction (XRD)

To determine the proper phase and complete morphology of any material, it is crucial to study its structural properties. The structural properties of a material are closely related to the chemical characteristics of the constituent particles of the material and thus form the foundation on which detailed physical understanding is built. Powder XRD is the most commonly used X-ray diffraction technique for characterizing polycrystalline materials by finding their crystal structure, atomic spacing, and unit cell dimensions [28-29]. The term 'powder' used in powder diffraction itself suggests that the material under study is in the powder form with randomly aligned fine grains of the crystalline material. XRD is an important technique for evaluating the properties of all kinds of matter ranging from fluids to powders and crystals. This technique is based on the principle of X-ray diffraction. The samples are typically in powder form, where ideally every possible crystalline orientation is represented equally. Diffraction of X-ray occurs when there is a constructive interference between the monochromatic beam of X-rays and the crystalline sample [30]. In the present study, all the powder samples were characterized by XRD patterns which were recorded by the powder XRD using a 1D PSD detector (LynxEye)

with Cu K_α radiation at room temperature. The structural studies of the samples and the phase identification are done by comparing the diffraction with the JCPDS (card number #) and previously reported delafossite oxides

B. X-ray Photoemission Spectroscopy (XPS)

X-ray photoelectron spectroscopy (XPS) is a surface characterization technique that can analyze a sample to a depth of 2 to 5 nanometers (nm). XPS reveals the presence of chemical elements at the surface and the nature of the chemical bond between elements. It delivers info about elemental composition, chemical state, thickness measurement of over layers of up to 8 nm on a substrate, surface chemical imaging, thickness and depth-distribution of chemical species and depth profiling the Valence Band photoelectron Spectroscopy (VBS). This also provides information on the density of states in the valence band and electron work function.

C. Vibrating Sample Magnetometer (VSM)

The measurement of the magnetic properties of any material is an important aspect mainly for understanding the mechanism of magnetic materials before fabricating the magnetic devices. The magnetic properties of the material are measured by Vibrating Sample Magnetometer (VSM) which was invented by Simon Foner at MIT Lincoln Laboratory in 1955 and reported in 1959 [31]. The study of magnetic properties of materials involves understanding the electronic behavior in condensed matter and material science. The electrons show highly correlated behavior i.e. the conduction electrons depend on the presence or absence of neighboring electrons in varieties of inorganic compounds and alloys of transition metals. These electronic correlations result in changes in material properties like magnetism, superconductivity, metal-insulator transitions, or heavy-fermion behaviour of conduction electrons. These behaviors are highly influenced by the Coulomb and exchange interactions among electrons. The working diagram of VSM is shown in Fig. 2.2.

The basic working principle of a VSM which provides information about the changing magnetic field is based on, Faraday's Law of induction, which tells us that the modification in the magnetic field produces a measurable electric field. The sample to be studied is kept in a constant uniform magnetic field. Superconducting Quantum Interference Device (SQUID) magnetometers are classified within the flux methods of measuring magnetization of a sample. This is useful to measure the small magnetic fields in the most sensitive way.

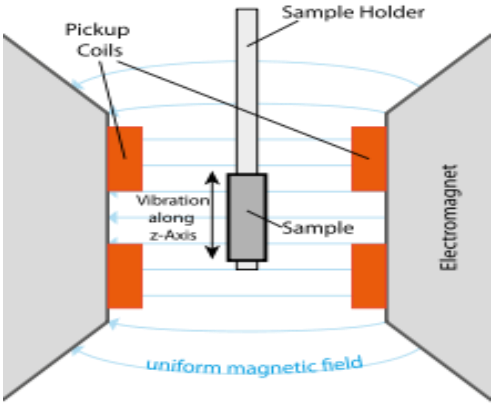

Figure 2.2: Schematic diagram depicting the working of vibrating sample magnetometer.

The electromagnet gets activated before the testing starts,hence, if the sample is magnetic, it will be magnetized and the stronger magnetic field is produced. This results in a magnetic field $\vec{H}$ around the sample. The magnetization of the specimen can be analyzed due to vibration in the sample as magnetization changes with the periodic movement. The changes in the magnetic flux prompt a voltage in the sensing coil proportional to the magnetization of the sample.

D. Raman spectroscopy

The Raman spectroscopy is the most common vibrational spectroscopic technique aimed at assessing the molecular vibrations and the bonding fingerprinting species principally based on inelastic scattering. When light scatters from an atom or crystal, most of the photons get scattered elastically and these scattered photons have the same energy and wavelength as that of the incident photons. However, a little fraction of light (approximately 1 in 107 photons)

is scattered at optical frequencies dissimilar from the frequency of the incident photons. This phenomenon of inelastic scattering is known as the Raman effect. Raman scattering takes place with a change in vibrational, rotational or electronic energy of the molecule. When the light in the form of electromagnetic radiation interacts with matter, the photons may get absorbed or scattered, or may simply pass through it without any interaction. If the energy of an incident photon is proportional to the energy gap between the ground state and an excited state, the system is promoted to a higher excited state after the photon is absorbed. It is this change which is measured in absorption spectroscopy. However, it is also possible for the photon to interact with the molecule and get scattered from it. The scattered beams of photons are observed by collecting light at an angle to the incident beam. In the case of Raman, scattering efficiency is directly proportional to the fourth power of the frequency of the incident light. In the present work, the Raman spectra were recorded by the micro Raman spectroscopy (STR 500, Nd-YAG laser source with 532 nm wavelength excitation laser). The recorded Raman spectra were analyzed using the Bilbao crystallographic server [32].

References

1. K. Schwarz, P. Blaha, S.B. Trickey, *Mol. Phys.* **108**, 3147 (2010).
2. Y. V Shtogun, L.M. Woods, G.I. Dovbeshko, *J. Phys. Chem. C*. **111**, 18174 (2007).
3. R.G. Parr, *in Horizons Quantum Chem.* (Springer Netherlands, Dordrecht, 1980), 5-15.
4. J.C. Slater, *New York, NY: McGraw-Hill*, 485 (1963).
5. E. Schrödinger, *Phys. Rev.* **28**, 1049 (1926).
6. M. Born, J.R. Oppenheimer, *Ann. Physik*. **84**, 457 (1927).
7. C.A. Coulson, *Rev. Mod. Phys*. **32**, 170 (1960).
8. F. Giustino, Materials Modelling Using Density Functional Theory: Properties and Predictions (Oxford University Press, 2014).
9. J.C. Slater, *Phys. Rev*. **36**, 57 (1930).
10. P. Hohenberg, W. Kohn, *Phys. Rev. B*. **136**, 864 (1964).
11. F. Bassani, F. Fumi, M.P. Tosi, Highlights of Condensed-Matter Theory (North-Holland, 1985).

12. W. Kohn, *Rev. Mod. Phys.* **71**, 1253 (1999).
13. W. Kohn, P. Vashishta, Phys. Solids Liq. Springr Science and Business Media (1983).
14. A.D. Becke, *Phys. Rev. A.* **33**, 2786, (1988).
15. P. Bagno, O. Jepsen, O. Gunnarsson, *Phys. Rev. B.* **40**, 1997 (1989).
16. S.Y. Savrasov, D.Y. Savrasov, and O.K. Andersen, *Phys. Rev. Lett.* **72**, 372 (1994).
17. P. Giannozzi, S. Baroni, N. Bonini, M. Calandra, R. Car, et al., *J. Phys. Condens. Matter.* **21**, 395502 (2009).
18. X. Gonze, *Phys. Rev. A.* **52**, 1096 (1995).
19. L.D. Landau, E.M. Lifshitz, J. B. Sykes, W. H. Reid, *Phys. Today*. **13**, 44 (1960).
20. F. Birch, *J. Appl. Phys*. **9**, 279 (1938).
21. M. Born, K. Huang, M. Lax, *Am. J. Phys*. **23**, 474 (1955).
22. J. Wang, S. Yip, S. R. Phillpot, D. Wolf, *Phys. Rev. Lett.* **71**, 4182 (1993).
23. Q. Hu, Q. Wu, Y. Ma, L. Zhang, Z. Liu, J. He, H. Sun, H.T. Wang, Y. Tian, *Phys. Rev. B.* **73**, 1 (2006).
24. A. Hao, X. Yang, X. Wang, R. Yu, X. Liu, W. Xin, and R. Liu, *Comput. Mater. Sci.* **108**, 063531 (2010).
25. R.C. Fang, Solid Spectroscopy, Chinese Science Technology University Press, Hefei 2003.
26. Y. Zhang, W. M. Shen, Basic of Solid Electronics, Zhe Jiang University Press, Hangzhou, 2005.
27. S. Saha, T. P. Sinha, A. Mookerjee, *Phys. Rev. B.* **62,** 8828 (2000).
28. A. R. West, Solid State Chemistry and its Applications, John Wiley and Sons, Chichester, New York, **20,** 492 (1984).
29. http://www.mrl.ucsb.edu/mrl/centralfacilities/xray/xray-basics/index.html
30. E. N. Kaufmann, Characterization of Materials, 2nd edition, John Wiley and Sons **3,** 1392 (2003).
31. S. Foner, *Rev. Sci. Instrum.* **30** 548 (1959).
32. E. Kroumova, M. I. Aroyo, J. M. Perez Mato, A. Kirov, C. Capillas, S. Ivantchev, H. Wondratschek *Phase Transitions*. **76**, 170 (2003).